Article:
Brunner, D., Burke, W., Kuang, A. Q. et al. (3 more authors) (2016) Feedback system for divertor impurity seeding based on real-time measurements of surface heat flux in the Alcator C-Mod tokamak. Review of Scientific Instruments. 023504. ISSN: 0034-6748

https://doi.org/10.1063/1.4941047

Feedback system for divertor impurity seeding based on real-time measurements of surface heat flux in the Alcator C-Mod tokamak

D. Brunner[1], W. Burke[1], A.Q. Kuang[1], B. LaBombard[1], B. Lipschultz[2], and S. Wolfe[1]

[1]*Plasma Science and Fusion Center, Massachusetts Institute of Technology, Cambridge, MA 02139 USA*

[2]*Department of Physics, University of York, Heslington, York, YO10 5DD, UK*

Mitigation of the intense heat flux to the divertor is one of the outstanding problems in fusion energy. One technique that has shown promise is impurity seeding, i.e., the injection of low-Z gaseous impurities (typically N_2 or Ne) to radiate and dissipate the power before it arrives to the divertor target plate. To this end the Alcator C-Mod team has created a first-of-its-kind feedback system to control the injection of seed gas based on real-time surface heat flux measurements. Surface thermocouples provide real-time measurements of the surface temperature response to the plasma heat flux. The surface temperature measurements are inputted into an analog computer that 'solves' the 1-D heat transport equation to deliver accurate, real-time signals of the surface heat flux. The surface heat flux signals are sent to the C-Mod digital plasma control system, which uses a PID algorithm to control the duty cycle demand to a pulse width modulated piezo valve, which in turn controls the injection of gas into the private flux region of the C-Mod divertor. This paper presents the design and implementation of this new feedback system as well as initial results using it to control divertor heat flux.

I. Introduction

The recent compilation of a multi-machine database on scrape-off layer heat flux widths has shed light on the heat flux challenge: the heat flux width scales inversely with the poloidal magnetic field and independent of machine size[1,2]. Such a scaling suggests that the unmitigated 'upstream' heat flux parallel to the magnetic field will be ~5GW/m^2 in ITER and ~10GW/m^2 in ARIES-class devices[3]. Active cooling technology[4] limits steady-state surface power exhaust to ~10MW/m^2. while erosion limits may require this to be even lower[3]. Tilting the divertor surface such that it is nearly parallel (~1°) to the magnetic field—such as in the vertical target plate divertor[5]—reduces the surface heat flux by a factor of ~60 from the parallel heat flux. This leaves a factor of ~10 gap in power handling.

One of the promising techniques to meet this heat flux handling gap is the injection of low-Z impurities[6], such as N_2 or Ne. Radiating impurities convert the plasma heat flux—which is essentially directed parallel to the magnetic field—into a more uniform photon heat flux, spreading the heat over a larger area. Low-Z impurities are efficient radiators of power (up to 10's MW/m^3) at temperatures (1-100eV) and densities (10^{20}-10^{21}m^{-3}) typical in the boundary plasma.

There have been many studies on radiative divertor seeding, primarily using feed-forward programming of the injection of impurities[7–9]. However, there is much less experience with feedback control of seeding. Experiments at JT-60[10] and Alcator C-Mod[11] have used the radiated power from a bolometer chord as the input to a feedback control of impurity injection. JET[12] has used a VUV nitrogen line for feedback control of nitrogen injection. ASDEX-U[13–15] has made extensive use of the current through a divertor tile (which is loosely tied to the divertor heat flux through reduction in the local electron temperature and thus the thermoelectric current[16]) as well as a double-feedback scenario[17], combining the tile current and a core bolometer channel to control the injection of efficient edge and core radiating impurities.

However, there has yet to be a heat flux mitigation feedback system controlled by the primary signal of interest: the surface heat flux. To this end, the Alcator C-Mod team has developed and implemented the first radiative divertor feedback control system with a surface heat flux input. C-Mod is an excellent environment to test such a system: it operates with the same high-Z vertical target plate divertor geometry as ITER and has boundary heat fluxes (~0.5-1.5GW/m^2) approaching those expected in ITER. This system uses molybdenum/tungsten-rhenium surface thermocouples[18] which directly expose the thermojunction to the plasma heat flux incident on the divertor. The surface thermocouple temperature is input into a simple analog RC computer that 'solves' the 1-D heat transport in a model of the surface thermocouple. The output of this analog computer is an accurate, real-time signal representative of divertor surface heat flux. The heat flux signal is used as the observer input into a PID controller implemented in the C-Mod Digital Plasma Control System (DPCS)[19]. Based on the error between the heat flux signal and a programmed observer level, the DPCS outputs a duty cycle set point voltage to a pulse width modulated piezo valve[20] introducing impurities into the divertor private flux region.

This paper proceeds as follows: Section II provides details of the new feedback system, including a review of the surface thermocouples as well as introductions to the heat flux calculation circuit, the piezo seeding valve and tube, and the PID controller implementation of the feedback system the DPCS. Section III demonstrates use of the system to control the divertor heat flux in Alcator C-Mod L-mode plasmas. A discussion of the feedback system and applicability to of such a technique to future systems is given in Section IV. Appendix A discusses improvements to the surface thermocouple system that have been made to the original surface thermocouples system described in Ref. [18]. Appendix B discusses how to extend the present surface thermocouple and heat flux circuit from a pulse system (~2s) to a steady-state system.

II. Feedback control system

a. Surface temperature measurements

Here we give a brief review of the surface thermocouple diagnostic. For a more detailed discussion of their implementation in C-Mod, see Ref. [18]. The surface thermocouples were custom made by NANMAC, based on their patented "self-renewing" thermocouple design[21]. The surface thermocouple is composed of a 2mm wide by 0.05mm thick 74% tungsten-26% rhenium ribbon that runs down the middle of a 6.35mm diameter molybdenum cylinder. The ribbon is electrically isolated from the cylinder with thin sheets of mica. The thermojunction is initiated on the plasma-facing surface by filing and cold welding the

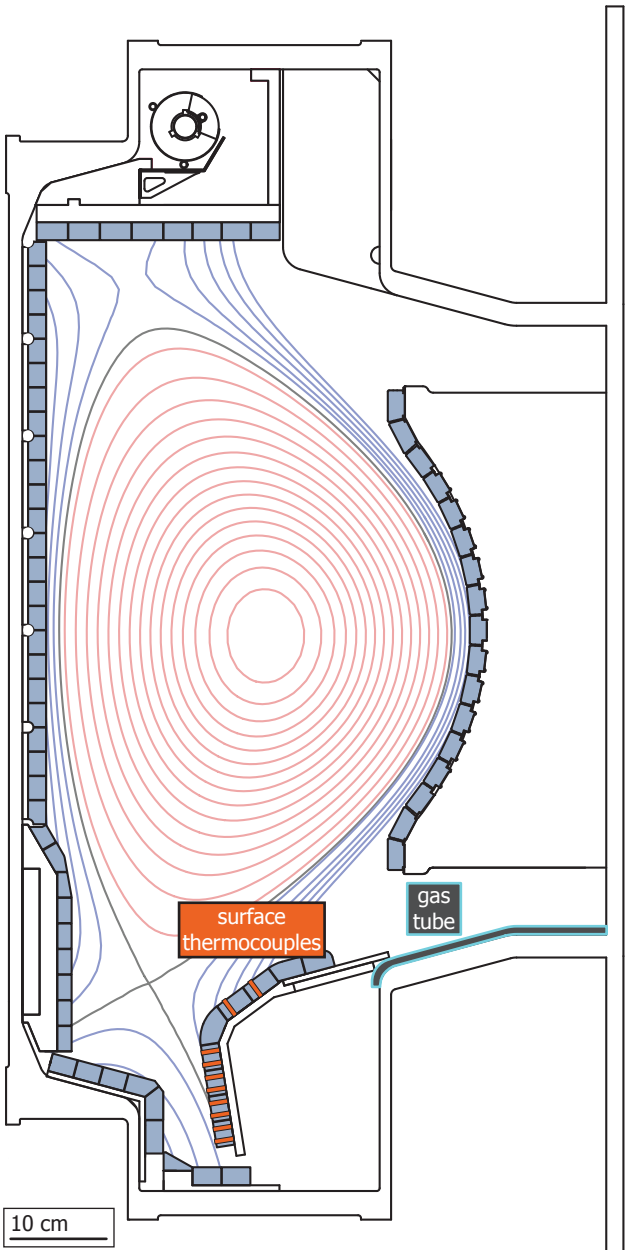

Figure 1 Cross section of Alcator C-Mod showing the location of the surface thermocouples in the outer divertor where the plasma heat flux is typically the largest and the gas tube injecting impurities in the "gas box" behind the divertor module. There is a gap at the bottom of the outer divertor that allows the gas to flow into the private flux region.

two thermoelectric elements. NANMAC supplied the non-linear voltage to temperature conversion (~16 μV/°C) for this non-standard thermojunction.

Signals are carried out on mineral insulated cables with copper center conductor and stainless steel cladding (coaxial cable was used in earlier implementations, we have subsequently switched to a triaxial cable to increase signal reliability, see Appendix A). As such, there are multiple uncompensated thermojunctions (e.g., tungsten-rhenium to copper and molybdenum to stainless steel) between the surface thermojunction and the measurement electronics. Use of this system therefore relies on making measurements of the ambient temperature of the thermocouple assembly prior to a discharge. This is performed via ice-point compensated type-K thermocouples embedded in the divertor tiles surrounding the surface thermocouples. The change in signal voltage during the plasma pulse is then attributed to a change in surface thermojunction voltage and thus surface temperature. This is a valid assumption during the discharges in C-Mod, which are too short (<2s) for the other thermojunctions to change temperature. Extension of this system to steady state is discussed in Appendix B. The surface heat flux is digitally computed after each plasma discharge by using the recorded surface temperatures as the boundary condition on 1-D finite element thermal model of the surface thermocouple.

An array of these surface thermocouples are mounted in the lower, outer divertor of Alcator C-Mod (see Figure 1 here as well as Fig. 1 in Ref. [22]) along with thermally isolated calorimeters and Langmuir probes. They are placed in a poloidal column of tiles that are ramped 2° with respect to the direction of the toroidal magnetic field. This ensures that the sensors are not shadowed by the adjacent divertor module. The integrated energy fluxes from the surface thermocouples were benchmarked against the calorimeters over all divertor plasma regimes—from sheath-limited to fully detached—demonstrating that they accurately measure the surface heat flux[18,23]. At low collisionality the profile of heat flux across the divertor had excellent agreement in comparison to Langmuir probe estimates of plasma heat flux using the standard sheath heat flux transmission coefficient modified to include finite current[18]. However they diverged as the divertor collisionality increased at the onset of divertor plasma pressure detachment, with the surface thermocouples reporting a much lower heat flux than expected from the Langmuir probes and sheath heat flux theory[24]. This discrepancy is a well-known and still outstanding issue in divertor plasma physics and probe interpretation[24,25]. Therefore, we choose to use surface thermocouples over Langmuir probes to generate the heat flux observer signal for this feedback system, largely due to the Langmuir probe's inability to accurately measure the divertor plasma parameters in this regime.

b. Real-time heat flux signal

The real-time heat flux calculation circuit takes advantage of the fact that heat diffusion through a solid and current diffusion through an RC network both have the same fundamental equations:

$$\frac{\partial T(x,t)}{\partial t} = \frac{\kappa}{\rho C_{\mathrm{p}}}\frac{\partial^2 T(x,t)}{\partial x^2}, \qquad \frac{\partial V(x,t)}{\partial t} = \frac{1}{R_{\mathrm{L}} C_{\mathrm{L}}}\frac{\partial^2 V(x,t)}{\partial x^2}. \tag{1}$$

Where T is the temperature, V voltage, κ is the thermal conductivity, ρ the mass density, C_{p} the heat capacity, R_{L} the resistance per unit length, and C_{L} the capacitance per unit length. Thus an RC transmission line can be used as an analog model for heat conduction. Applying the voltage output of the surface thermocouples as the input voltage boundary condition to the RC transmission line, the surface heat flux incident on the surface thermocouples is simply proportional to the current entering the RC transmission line. Modeling heat transport with analog circuits was common around the 1960's as it was much easier at the time to implement than numerical compuration[26]. Present day applications of the electrical analog technique to model heat conduction include interpretation of thin-film gauges[27] as well as thermal models for integrated circuits[28].

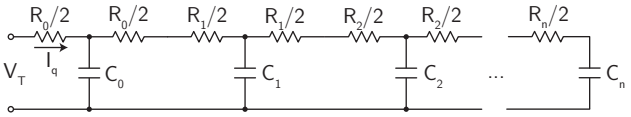

Figure 2 Schematic of the discrete RC transmission line used as an analog computer for real-time calculations of surface heat flux.

Although a continuous RC network with matched diffusivity to the molybdenum surface thermocouple body could produce a highly accurate analog thermal model, it is simpler and sufficient to use discrete electrical components, Figure 2. This is the physical equivalent to using a finite-element digital calculation as a numerical approximation to solving the diffusion equation. Using discrete components requires specification of the physical node spacing. Since this system must primarily simulate changes in surface heat fluxes, an optimized node spacing, Δx_{n}, has small spacing at the surface to accurately model steep gradients in the temperature. While larger node spacing towards the rear of the sensor model is sufficient to accurately model heat transport over long-time scales.

To find the minimum number of nodes and the optimal node spacing for pulsed surface heat fluxes we utilized the same finite element heat transport code used to compute surface heat fluxes from surface thermocouple data after plasma pulses. First a

run of the code with finely spaced nodes was done, applying a 10MW/m^2 heat pulse to the surface for 10s. The resulting surface temperature evolution was stored and then applied to a series of models with much sparser node spacing (from 3 to 15 nodes, holding the total length of the simulated body constant). To optimize the number of nodes and node spacing, the resulting surface heat flux calculations were then compared to the input on the first model. An error-minimization algorithm was allowed to adjust the node spacing for each case such that the simulated heat flux most closely matched original 10MW/m^2 10s pulse.

Using this technique, we found that a 7 node RC ladder with ~2.2 factor increase of Δx between adjacent nodes was able to accurately model (<5% error) heat fluxes spanning times scales from 1ms to 10s. This was sufficient to keep up with the thermal response of the surface thermocouples (few milliseconds) through the duration of a typical C-Mod pulse (~2 seconds). The optimal ~2.2 node spacing was fortunate, as standard capacitors are available in factor ~2.2 increments. The results were not particularly sensitive to the 2.2 value increase in node spacing. Increasing the number of nodes primarily results in finer node spacing at the surface, which increases the accuracy of the calculation at small time scales beyond what is necessary for this situation. Decreasing the number of nodes primarily results in larger node spacing at the surface, slowing down the time response of the calculation.

Thermal resistance and heat capacity of solids varies with temperature but the values of standard resistors and capacitors are independent of voltage. Consequently, fixed representative values of thermal properties of molybdenum had to be chosen. Using the properties at 100°C (ρ=10240kg/m^3, C_p=261J/kg/K, κ=134W/m/K, α=5e-5m^2/s) was a fair compromise, since the bulk of the surface thermocouple body is around this temperature through the course of a plasma discharge. This approximation results in small, few percent, underestimates of the surface heat flux at elevated temperatures. The values for our optimized node spacing and corresponding discrete resistor and capacitor values are shown in Table I. The capacitor values were chosen based on common values and the observation that the optimized node spacing increases by ~2.2. The resistor values were calculated from the optimized node spacing points and capacitor values ($R_n = \Delta x_n^2/\alpha C_n$). Comparison of the real-time analog and post-processed digital computations of surface heat flux are shown in Figure 3. In this plasma discharge auxiliary heating power was modulated, resulting in large modulations to the surface heat flux. The real-time analog computation matches both the magnitude and fast time scales of the surface heat flux modulations as well as the long-term evolution of the surface heat flux.

Table I Values of the optimized finite element node distances along with the corresponding resistances and capacitances.

T-node	0	1	2	3	4	5	6

Δx_n [mm]	0.240	0.240	0.513	1.09	2.40	5.13	10.9
R_n [kΩ]	5.22	5.22	11.2	23.8	52.2	112.	238.
C_n [μF]	0.220	0.220	0.470	1.00	2.20	4.70	10.0

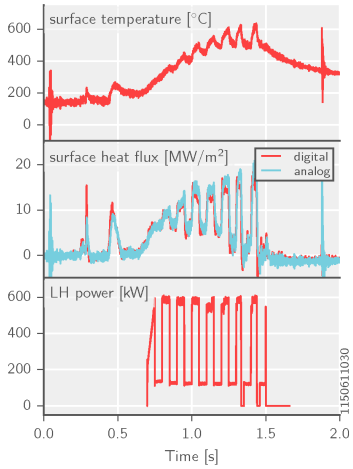

Figure 3 Comparison of the response of the real-time analog heat flux computer and the post-discharge digital computation during a plasma discharge where the Lower Hybrid (LH) auxiliary power was modulated. Top panel shows the surface temperature evolution, middle panel shows the analog (red) and digital (blue) computed heat fluxes, and bottom panel the modulated auxiliary power.

c. Divertor impurity seeding valve and tube

An impurity seeding valve and tube were installed principally for feedback control experiments. The seeding tube releases gas into the volume behind the lower, outer divertor module (Figure 1). The divertor modules have a gap underneath them that allows the seeding gas into the private flux region. A pulse width modulated piezo valve releases the seeding gas from a plenum into the seeding tube. The pressure of gas in the plenum sets the maximum seeding rate. Seeding rates below this value can be obtained by changing the demand voltage that controls the duty cycle of the pulse width modulation[20]. Typical plenum pressures for N_2 seeding range from ~15-45psi (~100-300Pa), total gas injected from ~5-10Torr-L (~0.67-1.3Pa-m^3), and time-averaged injection rates of ~10Torr-L/s (~1.3Pa-m^3/s).

d. PID controller

The C-Mod DPCS[19] is used as the control interface for this heat flux feedback system. Both the surface heat flux input signals and the duty cycle demand output signals are connected to the DPCS through Analog Fiber Optic Links (AFOLs) to maintain electric isolation of the separate systems. The DPCS allows for a straightforward implementation of a PID controller[29]. Before each discharge, independent waveforms may be programmed for each of the signals:

1. Surface heat flux demand set point
2. Duty cycle feed forward program
3. Proportional error coefficient
4. Integral error coefficient
5. Derivative error coefficient

The DPCS calculates the error of the inputted observer (real-time surface heat flux) with the set point signals and outputs a demand voltage to the valve duty cycle based on the feed forward programming and the sum of the proportional, integral, and derivative of the error multiplied by their respective coefficients. The DPCS controller also allows for more complex control algorithms to be programed (e.g., one based on a state-space model), however, this option was not implemented for this first instance of the heat flux feedback system.

III. Feedback control of surface heat flux in L-mode plasmas

L-mode plasmas are an excellent platform in which to test the heat flux feedback control system: they do not require auxiliary heating systems, are relativity steady and easy to obtain, have low impurity confinement in the core plasma and in C-Mod, and with high plasma current (1.1MA) can reach unmitigated boundary heat fluxes parallel to the magnetic field of ~0.5GW/m^2 (surface heat flux ~25MW/m^2 on the surface thermocouples). It was found that using the average of four of the surface thermocouples within 4mm of the strike point (mapped to the outer midplane along magnetic flux surfaces) provided a good input signal that minimized effect of moving strike point position. It was relatively straightforward to implement the PID controller, taking only a few discharges to tune up the P, I, and D gains to achieve a stable response. Not only is such a system an important test of the ability to mitigate surface heat flux in a controlled way, it also has proven useful in performing controlled experiments to systematically explore the effects radiation-based dissipation of divertor heat flux on the 'upstream' heat flux width. Use of the heat flux controller in high power H-mode plasmas will be reported in a future publication.

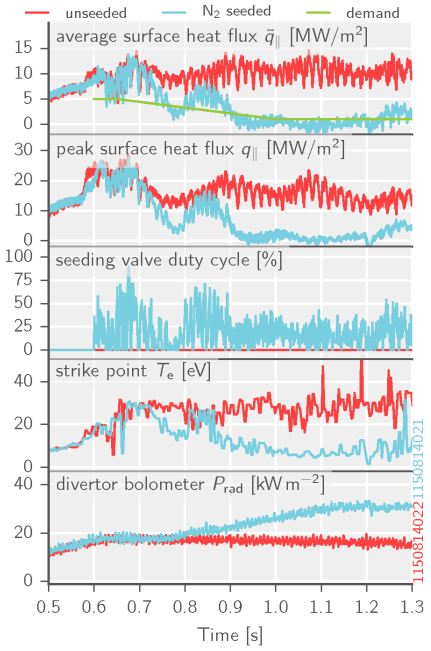

Figure 4 Demonstration of the heat flux feedback system. Red traces are from a plasma discharge with the heat flux feedback system off and blue traces are from a repeated discharge with it on. Top panel is the average of the surface heat flux from the four sensors nearest the strike point. Second panel is the surface heat flux from the sensor nearest the peak; due to the discrete sensors, the actual peak surface heat flux may not be measured.

IV. Discussion

This paper reports the first demonstration of feedback control of impurity seeding in a tokamak via direct measurement of divertor target surface heat flux. The system was found to provide controlled mitigation of large heat fluxes through injection of radiating impurities, similar to what has been achieved before in feed-forward impurity seeding experiments. Despite its utility, this type of system has inherent performance limitations. While adequate for steady or slowly changing heat fluxes, the system (and any system based on injection of neutral gas) is clearly not able to respond to fast timescale phenomena, such as those associated with plasma that occur faster than a ~100ms. The main limitation stems from the slow transport of injected gas from the valve, through the seeding tube, and into the plasma. The oscillation period of the PID controller (as

seen in Figure 4), which is a rough measure of the response time, is typically ~150ms. Feedback via gas seeding will be inadequate to deal with the time-changing heat fluxes through an ELM (Edge-Localized Mode[30]), i.e., large bursts of particles and heat to the boundary arriving in ~1ms timescale. Ideally, the impurity radiation front itself is resilient enough to absorb the transient heat and particle fluxes and keep the high heat flux from the ELMs from reaching the target. One promising possibility is to take advantage of the radiation front stability due to total flux expansion[3,31,32] (i.e., a divertor leg which extends out in major radius).

Another limitation is that the system only has an active 'push' of seeding gas into the system and has no controlled 'pull', relying instead on the passive pumping of nitrogen by the first wall as well as that by the cryopump. To avoid over-puffing the seeding gas—and possibly ruining the discharge—this lack of control restricts the peak gas input rate. Another option that is presently being explored is to use the C-Mod lower hybrid system (which is normally used to drive current in the core plasma) as an active 'pull' on the seeding by adding power to the boundary plasma. The lower hybrid system is shown to be a capable tool in this respect: it can put 100's of kW of power into the boundary within 1ms of turning on (Figure 3). On the other hand, heating systems that deposit their power in the core plasma (such as Ion-Cyclotron Range of Frequencies (ICRF) as used on C-Mod), change the divertor heat balance on core energy confinement timescales (>10ms on C-Mod). This is faster than the time response of neutral gas injection but still much slower than direct deposition of power in the boundary.

A heat flux feedback control system for impurity seeding such as that employed here could be readily extended to other devices. Means to extending the pulsed system used in C-Mod to long-pulse/steady-state systems are discussed in Appendix B. Although the survivability of many diagnostics within the neutron environment of a reactor remains to be demonstrated, if adequate insulators as well as thermoelements that are insensitive to transmutation under the fusion neutron spectrum are found, the surface thermocouple could be used as the heat flux sensor in burning plasma devices (e.g., ITER[33], DEMO[34], or ARC[35]). There has been some research into using standard thermocouples in a fusion nuclear environment for ITER[36]. Additionally, IR cameras or diodes may also be used as heat flux sensors (since the submission of this paper, work demonstrating the development of a real-time capable IR system for ASDEX-U has been publish[37]). Although IR-based systems must confront the challenges of making accurate measurements of surface heat flux in the presence of uncertainties in the surface emissivity[38], surface films, and thermal conductivity[25,39], they only require an optical pathway to the target surface. Finally, an analog heat flux computer was chosen because it was inexpensive and simple to build. However, digital computation of the surface heat flux from the surface temperature is also a viable method.

Acknowledgements

This research was done at the Alcator C-Mod tokamak, a DOE Office of Science user facility, supported by DOE Contract No. DE-FC02-99ER54512-CMOD. The research by B. Lipschultz was funded in part by both the Wolfson Foundation and UK Royal Society through a Royal Society Wolfson Research Merit Award as well as the RCUK Energy Programme [grant number EP/I501045]. Thanks to M. Reinke and I. Faust for the bolometer measurements. Thanks to R. Rosati for his craftsmanship in making the surface thermocouple cables.

Appendix A: Improvements to the surface thermocouple system

There have been three important improvements to the surface thermocouple system on C-Mod since the 2012 paper in RSI[18]. The first being the cabling: The original cabling system used mineral insulated coaxial cable (stainless steel clad with copper center conductor) with the tungsten-rhenium thermo-element attached to the center conductor and the molybdenum thermo-element attached to the cladding. Fiberglass cloth insulated the shield from grounding to the vacuum vessel. Through the course of a campaign, the cloth would wear away, shorting the cladding to the vacuum vessel, causing ground loops, and introducing electromagnetic noise to the signal. Beginning the FY2015 campaign, the coaxial cabling was replaced with triaxial cabling while the same thermo-element arrangement was maintained on the center conductor and inner shield. The outer shield of the triaxial cable replaced the fiberglass cloth, providing much more resilient protection against shorts to ground. Since this replacement there have been no such grounding failures. Triaxial cabling was previously not used in C-Mod due to concerns about virtual leaks from trapped volumes. However, tests of triaxial cable in a vacuum oven showed the outgassing rate to be sufficiently small to use in C-Mod.

Another improvement to the reliability of the surface thermocouples was to follow closely NANMAC's guidelines for initiating the surface thermojunction[40]. Before this, the thermocouple surfaces were filed flush to the divertor surface in a nearly random pattern at initial installation. Some sensors were found to fail as having an open circuit condition at some time during the course of an experimental campaign. For the FY2015 campaign we followed NANMAC's guideline of filing the surface thermojunction only in one direction, going across the ribbon at ~45° angle. This technique forms a solid thermojunction through friction welding the thermoelements at the surface. Since implementing this technique, the occurrence of open circuits has been significantly reduced. However, open circuits have occurred in discharges where the surface temperature is very large (~2000K), perhaps due to thermal expansion breaking open the thermojunction. True to their 'self-renewing' name, the thermojunctions on these sensors reformed in later discharges when under less intense conditions.

The final improvement made surface thermocouple measurements possible during high ICRF power – a key to enabling high heat flux feedback experiments in C-Mod. Previously RF pickup had precluded the use of surface thermocouples during ICRF operation[18]. The original installation of the surface thermocouple system had feedthroughs with ceramic breaks to electrically isolate the cladding of the coaxial cable from the vacuum vessel. Since then, the feedthroughs have been modified to provide an open circuit for DC but a short circuit at RF frequencies. Copper foil is wrapped around the ceramic break, grounded to the feedthrough on one side and electrically isolated by Kapton tape on the other. This RF-short has effectively eliminated all RF pickup during ICRF operation.

Appendix B: Extension of surface thermocouple measurements to a long pulse system

The surface thermocouple system and analog heat flux computation circuit were designed for the pulsed environment of C-Mod. That is, the discharge length in C-Mod is short enough to assume that only the surface thermojunction changes temperature and the rear of the surface thermocouple (~20mm from the surface) does not change temperature. This allows for the surface thermocouple signal to be carried on wires made from metals other than the thermocouple pair. However, surface thermocouples could easily be designed for long pulse or continuous systems where the temperature at the rear of the surface thermocouple would change. There are two options for a long pulse system: 1. Continue the thermo-element pair all the way from the thermojunction to the measurement electronics. This would be possible using standard thermo-element pairs using combinations of tungsten and rhenium (e.g., thermocouple types C, D, or G). 2. Carry the signal out on a matched pair of wires (most likely copper) and measure the temperature of the (reference) junction where the thermocouple pair meets the matched pair.

Another change going to long pulse would be the boundary condition at the rear of the thermal model. The two boundary conditions for the pulsed model on the analog heat flux computer are the temperature on the front surface (from the surface thermocouple) and an assumption of zero heat flux on the back surface. Zero heat flux is an adequate assumption given the long length of the surface thermocouple and short time of the plasma discharge. A long pulse system would need a different rear boundary condition. The most likely option would be to have another thermocouple embedded behind the surface and placing that temperature as the rear boundary condition on an appropriate analog model of this new system. This situation would work well with the second option for modifying the surface thermocouple cabling for long pulse: the temperature measurement of the reference junction would make an appropriate rear thermal boundary condition.

References

[1] T. Eich, A.W. Leonard, R.A. Pitts, W. Fundamenski, R.J. Goldston, T.K. Gray, A. Herrmann, A. Kirk, A. Kallenbach, O. Kardaun, A.S. Kukushkin, B. LaBombard, R. Maingi, M.A. Makowski, A. Scarabosio, B. Sieglin, J. Terry, and A. Thornton, Nucl. Fusion **53**, 093031 (2013).

[2] M.A. Makowski, D. Elder, T.K. Gray, B. Labombard, C.J. Lasnier, A.W. Leonard, R. Maingi, T.H. Osborne, P.C. Stangeby, J.L. Terry, and J. Watkins, Phys. Plasmas **19**, 056122 (2012).

[3] B. LaBombard, E. Marmar, J. Irby, J.L. Terry, R. Vieira, G. Wallace, D.G. Whyte, S. Wolfe, S. Wukitch, S. Baek, W. Beck, P. Bonoli, D. Brunner, J. Doody, R. Ellis, D. Ernst, C. Fiore, J.P. Freidberg, T. Golfinopoulos, R. Granetz, M. Greenwald, Z.S. Hartwig, A. Hubbard, J.W. Hughes, I.H. Hutchinson, C. Kessel, M. Kotschenreuther, R. Leccacorvi, Y. Lin, B. Lipschultz, S. Mahajan, J. Minervini, R. Mumgaard, R. Nygren, R. Parker, F. Poli, M. Porkolab, M.L. Reinke, J. Rice, T. Rognlien, W. Rowan, S. Shiraiwa, D. Terry, C. Theiler, P. Titus, M. Umansky, P. Valanju, J. Walk, A. White, J.R. Wilson, G. Wright, and S.J. Zweben, Nucl. Fusion **55**, 053020 (2015).

[4] M.S. Tillack, A.R. Raffray, X.R. Wang, S. Malang, S. Abdel-Khalik, M. Yoda, and D. Youchison, Fusion Eng. Des. **86**, 71 (2011).

[5] B. Lipschultz, B. LaBombard, J.L. Terry, C. Boswell, and I.H. Hutchinson, Fusion Sci. Technol. **51**, 369 (2007).

[6] A. Kallenbach, M. Bernert, R. Dux, L. Casali, T. Eich, L. Giannone, A. Herrmann, R. McDermott, A. Mlynek, H.W. Müller, F. Reimold, J. Schweinzer, M. Sertoli, G. Tardini, W. Treutterer, E. Viezzer, R. Wenninger, and M. Wischmeier, Plasma Phys. Control. Fusion **55**, 124041 (2013).

[7] J.W. Hughes, A. Loarte, M.L. Reinke, J.L. Terry, D. Brunner, M. Greenwald, A.E. Hubbard, B. LaBombard, B. Lipschultz, Y. Ma, S. Wolfe, and S.J. Wukitch, Nucl. Fusion **51**, 083007 (2011).

[8] R. Neu, K. Asmussen, and K. Krieger, Plasma Phys. Control. Fusion **165**, (1996).

[9] C. Giroud, G. Maddison, K. McCormick, M.N.A. Beurskens, S. Brezinsek, S. Devaux, T. Eich, L. Frassinetti, W. Fundamenski, M. Groth, A. Huber, S. Jachmich, A. Järvinen, A. Kallenbach, K. Krieger, D. Moulton, S. Saarelma, H. Thomsen, S. Wiesen, A. Alonso, B. Alper, G. Arnoux, P. Belo, A. Boboc, A. Brett, M. Brix, I. Coffey, E. de la Luna, D. Dodt, P. De Vries, R. Felton, E. Giovanozzi, J. Harling, D. Harting, N. Hawkes, J. Hobirk, I. Jenkins, E. Joffrin, M. Kempenaars, M. Lehnen, T. Loarer, P. Lomas, J. Mailloux, D. McDonald, A. Meigs, P. Morgan, I. Nunes, C. Perez van Thun, V. Riccardo, F. Rimini, A. Sirinnelli, M. Stamp, and I. Voitsekhovitch, Nucl. Fusion **52**, 063022 (2012).

[10] N. Asakura, T. Nakano, N. Oyama, T. Sakamoto, G. Matsunaga, and K. Itami, Nucl. Fusion **49**, 115010 (2009).

[11] J.A. Goetz, B. LaBombard, B. Lipschultz, C.S. Pitcher, J.L. Terry, C. Boswell, S. Gangadhara, D. Pappas, J. Weaver, B. Welch, R.L. Boivin, P. Bonoli, C. Fiore, R. Granetz, M. Greenwald, A. Hubbard, I. Hutchinson, J. Irby, E. Marmar, D. Mossessian, M. Porkolab, J. Rice, W.L. Rowan, G. Schilling, J. Snipes, Y. Takase, S. Wolfe, and S. Wukitch, Phys. Plasmas **6**, 1899 (1999).

[12] G.P. Maddison, C. Giroud, G.K. McCormick, B. Alper, G. Arnoux, P.C. da Silva Aresta Belo, M.N.A. Beurskens, A. Boboc, A. Brett, S. Brezinsek, I. Coffey, S. Devaux, P. Devynck, T. Eich, R. Felton, W. Fundamenski, J. Harling, A. Huber, S. Jachmich, E. Joffrin, P.J. Lomas, P. Monier-Garbet, P.D. Morgan, M.F. Stamp, G. Telesca, H. Thomsen, and I. Voitsekhovitch, Nucl. Fusion **51**, 082001 (2011).

[13] A. Kallenbach, R. Dux, J.C. Fuchs, R. Fischer, B. Geiger, L. Giannone, A. Herrmann, T. Lunt, V. Mertens, R. McDermott, R. Neu, T. Pütterich, S. Rathgeber, V. Rohde, K. Schmid, J. Schweinzer, and W. Treutterer, Plasma Phys. Control. Fusion **52**, 055002 (2010).

[14] A. Kallenbach, P.T. Lang, R. Dux, C. Fuchs, A. Herrmann, H. Meister, V. Mertens, R. Neu, T. Pütterich, and T. Zehetbauer, J. Nucl. Mater. **337-339**, 732 (2005).

[15] J. Schweinzer, a. C.C. Sips, G. Tardini, P. a. Schneider, R. Fischer, J.C. Fuchs, O. Gruber, J. Hobirk, a. Kallenbach, R.M. McDermott, R. Neu, T. Pütterich, S.K. Rathgeber, J. Stober, and J. Vicente, Nucl. Fusion **51**, 113003 (2011).

[16] A. Kallenbach, A. Carlson, G. Pautasso, A. Peeters, U. Seidel, and H. Zehrfeld, J. Nucl. Mater. **293**, 639 (2001).

[17] A. Kallenbach, M. Bernert, T. Eich, J.C. Fuchs, L. Giannone, A. Herrmann, J. Schweinzer, and W. Treutterer, Nucl. Fusion **52**, 122003 (2012).

[18] D. Brunner and B. LaBombard, Rev. Sci. Instrum. **033501**, 033501 (2012).

[19] J.A. Stillerman, M. Ferrara, T.W. Fredian, and S.M. Wolfe, Fusion Eng. Des. **81**, 1905 (2006).

[20] R. Tesfaye, W.M. Burke, G.L. Dekow, and T.L. Toland, in *Fusion Eng. (SOFE), 2013 IEEE 25th Symp.* (San Francisco, CA, 2013), pp. 1–4.

[21] J. Nanigian and D. Nanigian, Proc. SPIE **6222**, 622203 (2006).

[22] B. LaBombard, J. Terry, and J. Hughes, Phys. … **056104**, 1 (2011).

[23] D. Brunner, Development of Probes for Assessment of Ion Heat Transport and Sheath Heat Flux in the Boundary of the Alcator C-Mod Tokamak, PhD Thesis, Massichusetts Institute of Technology, 2013.

[24] D. Brunner, M. Umansky, B. Labombard, and T. Rognlien, J. Nucl. Mater. 1 (2013).

[25] J. Marki, R. Pitts, T. Eich, and A. Herrmann, J. Nucl. Mater. **365**, 382 (2007).

[26] G.T. Skinner, *Analog Network to Convert Surface Temperature to Heat Flux* (1960).

[27] W.K. George, W.J. Rae, and S.H. Woodward, 333 (1991).

[28] V. Székely, A. Poppe, A. Páhi, A. Csendes, G. Hajas, and M. Rencz, IEEE Trans. Very Large Scale Integr. Syst. **5**, 258 (1997).

[29] A. O'Dwyer, *Handbook of PI and PID Controller Tuning Rules* (Imperial College Press, London, 2009).

[30] P.B. Snyder, H.R. Wilson, J.R. Ferron, L.L. Lao, A.W. Leonard, T.H. Osborne, A.D. Turnbull, D. Mossessian, M. Murakami, and X.Q. Xu, Phys. Plasmas **9**, 2037 (2002).

[31] I.. Hutchinson, Nucl. Fusion **34**, 1337 (1994).

[32] B. Lipschultz, F.I. Parra, and I.H. Hutchinson, Submitt. to Nucl. Fusion (n.d.).

[33] B.J. Green, Plasma Phys. Control. Fusion **45**, 687 (2003).

[34] S. Konishi, S. Nishio, and K. Tobita, Fusion Eng. Des. **63-64**, 11 (2002).

[35] B.N. Sorbom, J. Ball, T.R. Palmer, F.J. Mangiarotti, J.M. Sierchio, P. Bonoli, C. Kasten, D. a. Sutherland, H.S. Barnard, C.B. Haakonsen, J. Goh, C. Sung, and D.G. Whyte, Fusion Eng. Des. (2015).

[36] R. Van Nieuwenhove and L. Vermeeren, Rev. Sci. Instrum. **75**, 75 (2004).

[37] B. Sieglin, M. Faitsch, A. Herrmann, B. Brucker, T. Eich, L. Kammerloher, and S. Martinov, Rev. Sci. Instrum. **86**, 113502 (2015).

[38] J.L. Terry, B. Labombard, D. Brunner, J. Payne, and G.A. Wurden, in *Rev. Sci. Instrum.* (2010), pp. 2–5.

[39] A. Hermann, 28th EPS Meet. ECA 1 (2001).

[40]Http//www.nanmac.com/documents/eroding-Thermocouple-Maintenance.pdf, Date Accessed 9-3-2015 (n.d.).